A LiNbO3 substrate surface acoustic wave microfluidic chip for patterning of cardiomyocytes

YongKang Li
School of Mechanical Engineering
Xi'an Jiaotong University
Xi'an China
lyk2019@ stu.xjtu.edu.cn

TengFei Zheng†
School of Mechanical Engineering
Xi'an Jiaotong University
Xi'an China
†tengfz@xjtu.edu.cn

ChangFeng Jia
School of Mechanical Engineering
Xi'an Jiaotong University
Xi'an China
jcfeng@stu.xjtu.edu.cn

AnPei Li
School of Mechanical Engineering
Xi'an Jiaotong University
Xi'an China
1261184181@qq.com

Richard Fu
Department Name
Institution/University Name
City State Country
email@email.com

ABSTRACT

Cardiovascular diseases continue to threaten human life, health and safety. Among various treatment methods, myocardial tissue engineering is one of the important methods to solve the problem of cardiovascular disease. The main goal of myocardial tissue engineering is to make the synthesized or repaired myocardial tissue have the original physiological function, and patterning the myocardial cells to form a certain regular directional arrangement is one of the most challenging techniques. Therefore, in this study, a surface acoustic wave microfluidic chip with LiNbO3 as the piezoelectric substrate was designed to meet the needs of patterned arrangement of cardiomyocytes.

This study introduces the preparation method of the microfluidic chip based on LiNbO3. The microfluidic chip is used to carry out the patterning simulation experiment of cardiomyocytes, and it is verified that the surface acoustic wave can make the silica particles oriented in the flow channel. The micro-channel is used to simulate the growth environment of cardiomyocytes. Analyzing the experimental results, it is concluded that the surface acoustic wave microfluidic chip designed in this study has patterned particles, demonstrating its application potential for repairing the surface of damaged parts of myocardial tissue. Finally, a surface acoustic wave microfluidic chip based on LiNbO3 was used to arrange cardiomyocytes in the hydrogel. Scanning the solidified myocardial fibers, it is concluded that the directional arrangement of the internal myocardial cells of the myocardial fibers obtained from the experiment is consistent with the theory. Demonstrated the huge application potential of LiNbO3 substrate surface acoustic wave microfluidic chip for cardiomyocyte patterning in myocardial tissue engineering.

CCS CONCEPTS

•Hardware~Hardware validation~Functional verification •Applied computing~Life and medical sciences~Consumer health

KEYWORDS

LiNbO3 substrate, microfluidic chip, surface acoustic wave, cardiomyocyte, patterning

1 Introduction

The heart plays the role of circulating blood to the organs of the whole body, transporting oxygen and nutrients, and taking away metabolites. It is very important in the human body. Worldwide, cardiovascular disease is the primary disease affecting human morbidity and mortality [1]. During embryonic growth and development, cardiomyocytes are highly differentiated and cannot regenerate [2]. Therefore, when myocardial cells are injured, in order to maintain the function of the heart to supply blood to the body's organs, the injured part can only be repaired and filled by the rapid proliferation of myocardial fibroblasts. However, the scar formed only fills the volume of the damaged site and does not have the original function. This will damage the function of the myocardium and even lead to heart failure. Heart transplantation is the main treatment for advanced cardiovascular disease, but this method is not universally applicable because it may cause consequences such as a lack of donors, complications caused by immunosuppressants, and transplant organ failure.

The proposal and development of the concept of tissue engineering has made it possible for humans to recreate various tissues and organs with corresponding functions. Myocardial tissue engineering has also become an important method for repairing a failing heart. The current myocardial tissue engineering can form myocardial tissue by transplanting cells in vivo, or inoculating cells on suitable scaffold materials to rebuild myocardial tissue by transplanting cells in vitro. Myocardial tissue is a cell structure composed of highly repeating units of similar cells. The arrangement of myocardial cells has a certain directionality, and they communicate effectively in a cooperative manner to perform specific functions [3]. For myocardial tissue cultured in vitro, the cells need to be patterned, which is essential for the development and function of the tissue [4]. Therefore, driving the directional patterned arrangement of cardiomyocytes in the scaffold is an important technology in myocardial tissue engineering, and it may even cause the myocardial tissue to produce more physiological

functions. However, due to the very small size of cardiomyocytes, a very high-precision size control method is required. In addition, the patterning of cardiomyocytes needs to meet the requirements of fast speed, high throughput, low consumption, and mass production, which poses challenges to many driving methods. Surface acoustic wave has been rapidly developed in scientific research today because of its high biocompatibility [5] [6], non-contact, high integration, strong control, low cost, mass production [7], etc. The advantage is very suitable for the patterning operation of cardiomyocytes in myocardial tissue [8], and it has the potential to promote the progress of myocardial tissue engineering research and application. Therefore, it is of great research significance to use surface acoustic wave technology to pattern myocardial cells inside myocardial tissue and to meet its specific requirements.

2 Analysis of patterning principle and design of surface acoustic wave device

2.1 The principle of surface acoustic wave generation

The surface acoustic wave is a mechanical wave that propagates in a certain direction, which is generated after the inverse piezoelectric effect converts the alternating electrical energy into mechanical energy when an oscillating electrical signal matching the resonant frequency is applied to the interdigital transducer. Surface acoustic waves can only propagate on the solid surface, and most of the energy is concentrated in the depth below the surface within a range of about a few wavelengths . The surface acoustic wave device used in this study is composed of a piezoelectric substrate and an interdigital transducer. The schematic diagram of the structure is shown in Figure 1. Among them, this study selected a 128°YX-direction lithium niobate substrate with the best acoustic effect as the piezoelectric material of the surface acoustic wave chip[9]. The interdigital transducers at both ends of the surface acoustic wave device transmit the input electrical signal to the surface acoustic wave through the inverse piezoelectric effect, and form a standing wave field in the micro flow channel between the two for particle arrangement.

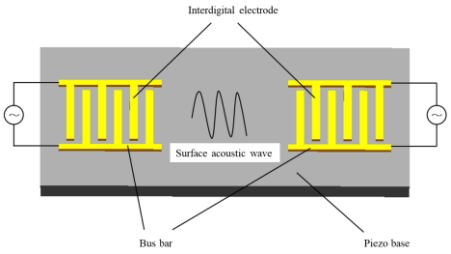

Figure 1 The composition of a surface acoustic wave device

2.2 Patterning principle

2.2.1 Principle of Standing Wave

Simultaneous application of radio frequency signals to excite a pair of identical and opposite interdigital transducers on the LiNbO3 piezoelectric substrate can generate two oppositely propagating surface acoustic waves, and the generated acoustic waves have the same frequency, opposite propagation directions, and maintain phase difference Constant. Two sound waves are refracted into the fluid at the angle of the Rayleigh angle, and interfere in the micro channel to form a composite wave with the position of the node and the antinode unchanged, which is the surface acoustic wave standing wave, as shown in Figure 2 (a). Taking a pair of incident wave and reflected wave as an example, assuming that there is no attenuation during reflection, the incident wave and reflected wave are respectively

$$F_a = -\left(\frac{\pi p_0^2 V_p \beta_l}{2\lambda}\right)\varphi(\beta,\rho)\sin(2kx) \tag{1}$$

$$y_2 = A\sin(kx+\omega t) \tag{2}$$

its synthetic wave is

$$\begin{aligned} y_1 + y_2 &= A\sin(kx-\omega t) + A\sin(kx+\omega t) \\ &= 2A\cos(\omega t)\sin(kx) \end{aligned} \tag{3}$$

In the formula, x=nπ/k (n ∈ Z) is the standing wave node position, and x=(nπ+π/2)/k (n∈Z) is the standing wave antinode position.

Figure 2(b) is a one-dimensional schematic diagram of the surface acoustic wave standing wave in the micro-channel, where the brighter part is the standing wave node, that is, the position where the energy is the lowest in the propagation of the sound wave; The darker part is the antinode of the standing wave, where the sound wave has a larger amplitude and energy. There is a λ/2 interval between adjacent nodes or antinodes. The cells or particles in the standing wave field will be pushed to the nodes or antinodes according to their own density and compressibility, forming a certain arrangement pattern.

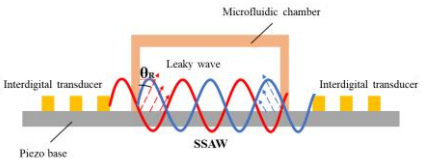

(a) Formation of standing waves

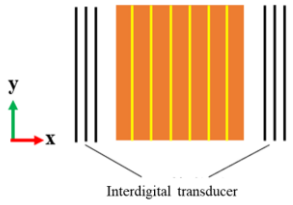

(b) Characteristics of standing wave field

Figure 2 Schematic diagram of standing wave

2.2.2 Force analysis of particles in SSAW

In the standing wave field, the acoustic force received by the microparticles is mainly the acoustic radiation force Fa, as shown in Figure3. Among them, Fax is the axial component of the acoustic radiation force, Fay is the lateral component, and FB is the force between the particles. The axial force is greater than the lateral force along the direction of sound wave propagation.

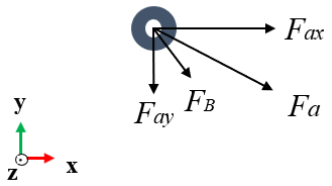

Figure 3 Schematic diagram of sound radiation force

The axial force component pushes the microparticles to the node of the standing wave, while the lateral force component gathers the microparticles together and restricts their position. The formula of axial radiation force Fa shows that the acoustic force is proportional to the square of the amplitude of the sound wave and the volume of the particle, as shown below:

$$F_a = -\left(\frac{\pi p_0^2 V_p \beta_l}{2\lambda}\right)\varphi(\beta,\rho)\sin(2kx) \tag{4}$$

$$\varphi = \frac{5\rho_p - 2\rho_l}{2\rho_p + \rho_l} - \frac{\beta_p}{\beta_L} \tag{5}$$

$$p_0 = \sqrt{\alpha \frac{p_{in}\rho_s c_s}{A_w}} \tag{6}$$

In the formula, F_a—— acoustic radiation force/N; V_p—— particle volume/m^3; λ—— wavelength/m; x—— distance between particle and PN/m; k—— wave number; p0—— sound pressure/Pa ; φ —— acoustic contrast factor; ρ_l—— density of medium/kg•m^{-3}, ρ_p—— density of particles/kg•m^{-3}; β_l—— compressibility of medium; β_p—— compressibility of particles; p_0—— sound pressure/Pa; α—— power conversion factor; p_{in}—— input power/W; ρ_s—— density of substrate/ kg•m^{-3}; c_s—— surface acoustic wave propagation velocity/m•s^{-1}; A_w—— working area of interdigital transducer/m^2.

This article first selects 5μm silica microspheres (Silica) particles to simulate the movement and arrangement of cardiomyocytes in a standing wave field.

2.3 IDT design and characteristic analysis of lithium niobate devices

a) Interdigital width a and inter-finger distance b

When the piezoelectric substrate material does not change, the acoustic wave wavelength λ is inversely proportional to the frequency f, and the interdigital width a of the IDT and the inter-finger distance b are equal, which are both a quarter of the wavelength λ. The wave velocity on the LiNbO3 substrate is v_s=3996m/s. Set the frequency of the surface acoustic wave device to f_0=25MHz, then the surface acoustic wave wavelength λ=159.84μm. In order to make the interdigital easier to make, rounded to λ=160μm, then the interdigital width a and the inter-finger distance b are both 40μm. From the previous analysis, it is known that the theoretical spacing of the patterned straight lines at this wavelength is 80 μm, which meets the range required for the arrangement of cardiomyocytes.

b) Interdigital logarithm N

To a certain extent, the greater the N, the greater the SAW intensity generated. However, when N is too much, the SAW generated between the interdigital fingers will interfere with each other to reduce the intensity and the stability of the waveform, and the frequency response bandwidth of the IDT will be narrowed, and SAW cannot be generated normally. Therefore, under comprehensive consideration, the number of interdigital transducer pairs N on the LiNbO3 chip is 20 pairs.

c) Acoustic aperture W

After determining the piezoelectric material and the number of interdigital fingers N, the input impedance of the IDT is completely determined by the acoustic aperture W. The acoustic aperture W not only affects the input impedance, but also has a certain impact on SAW diffraction. Under comprehensive consideration, the IDT's aperture W is 9.8mm.

d) Characteristic analysis

The characteristic frequency of 24.3MHz is obtained through the frequency sweep analysis of the microfluidic chip on the lithium niobate substrate, and the surface acoustic wave has the highest energy and the largest amplitude at this characteristic frequency.

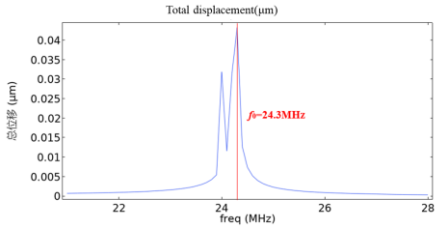

Figure 4 Interdigital center amplitude diagram

3 Simulation analysis of cell patterning driven by surface acoustic wave devices

In this section, a LiNbO3 based microfluidic chip is used to explore the influence of different microchannel angles on the cell/particle arrangement. In this experiment, a cylindrical glass tube is used as a micro-channel for simulation. Suppose the angle between the axis of the glass tube and the interdigital transducer is θ, the simulation includes a total of 10 groups, and the angle θ increases from 0° to 90° in sequence. The schematic diagram is shown in Figure 5.

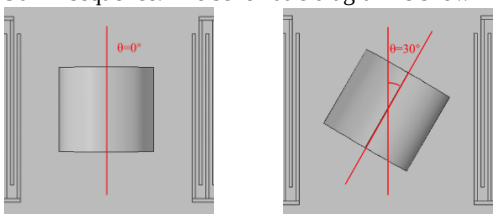

（a）θ=0°　　（b）θ=30°

Figure 5 Schematic diagram of rotation angle θ

Part of the simulation results is shown in Figure6.

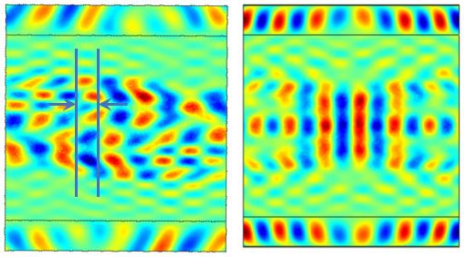

（a）θ=45°　　（b）θ=90°

Figure 6 The distribution of sound pressure in the tube at different positions of the microtubules

Among them, the red and blue areas represent the antinodes of the sound wave; The green part between the red area and the blue area represents the nodes, and the cells or particles will be patterned and arranged at the nodes. From the sound pressure distribution of multiple sets of simulation results, it can be seen that when the angle θ between the axis of the glass tube and the interdigital transducer is 0° to 20°, the cells/particles are arranged at the nodes, resulting in The linear pattern will be parallel to the tube wall; When θ is 20° to 30°, the patterned straight line will gradually evolve from the direction parallel to the tube wall to perpendicular to the tube wall; at 30° to 90°, the cells/particles will be arranged perpendicular to the tube wall.

The patterned arrangement of cells or particles in the experiment can be estimated by measuring the distance between the nodes on the cross section. The average distance between the nodes corresponding to different θ and the maximum value graph obtained by measurement are shown in Figure 7. The distance between the nodes in the figure is generally around 80 μm, which corresponds to half of the wavelength of the surface acoustic wave device.

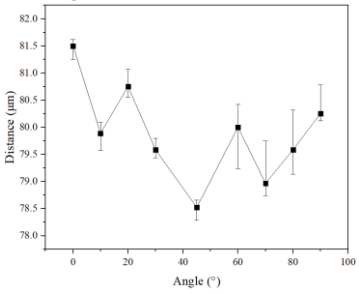

Figure 7 Corrugation pitch in the tube

4 Patterning experiment and result analysis

In this study, a lithium niobate surface acoustic wave microfluidic chip was designed and fabricated based on the simulation results. The chip was used to explore the patterning effect of cardiomyocytes. The experimental verification and summary of the patterning ability of cardiomyocytes were carried out by changing the angle of the microchannels.

4.1 Preparation of microfluidic chip

In the study, the mask was first designed according to the aforementioned interdigital parameters, and then the microfluidic chip was prepared according to the process shown in Figure 8.

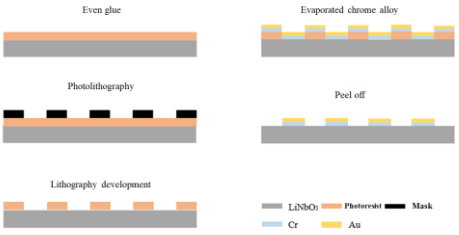

Figure 8 production process

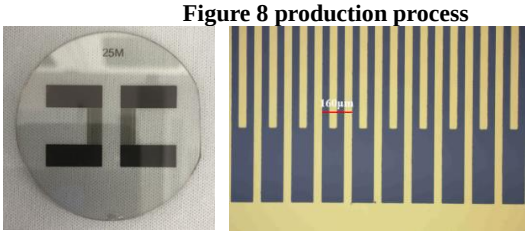

(a) Physical image of rigid chip
(b) Partially enlarged image
Figure 9 Microfluidic chip based on LiNbO3

4.2 Experimental verification and analysis

When verifying the patterning effect of the microfluidic chip, a lithium niobate chip with a characteristic frequency of 24.3MHz was used, and a 5μm silica particle suspension was injected into the glass capillary tube using a syringe. Set deionized water as the coupling agent between a pair of interdigital fingers on the chip, and place the glass capillary tube on the coupling agent. When the 24.3MHz, 30mV and amplified signal is applied to the interdigital transducer, the silica particles in the cylindrical glass microtubes are quickly arranged in a linear pattern, as shown in Figure 10.

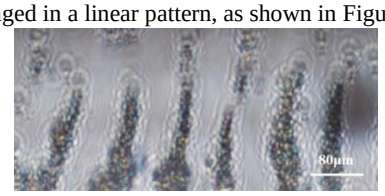

Figure 10 Particle patterning in the tube

By changing the size of θ to explore the influence of the position of the micro-channel relative to the interdigital transducer on the standing wave field and the patterned arrangement of cardiomyocytes or particles, as shown in Figure 11.

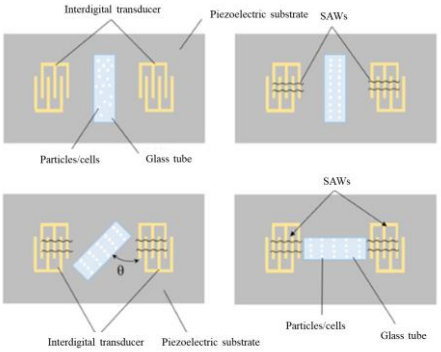

Figure 11 Schematic diagram of the experiment

In the experiment, multiple sets of experimental verification were carried out by changing the size of θ from 0° to 90°, and some of the results obtained are shown in Figure 12.

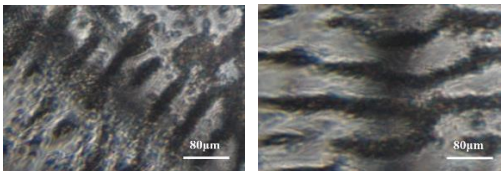

（a）45°　　（b）90°

Figure 12 Particle arrangement on the rigid chip when changing the position of the micro flow channel

Conclusions can be drawn from the experimental results: When the angle θ between the glass microtube and the interdigital transducer is 0° and 90°, the patterned line of the silica particles is parallel to the interdigital direction, which is consistent with the traditional patterning phenomenon in Figure 11. But when θ is 45°, the straight line patterned by the silica particles is perpendicular to the wall of the glass tube and forms an angle of 45° with the interdigital direction. The simulation results of this arrangement phenomenon are consistent with the theory, and this phenomenon will bring more value in the future exploration of microfluidic chips for the patterning of cardiomyocytes.

4.3 Microfluidic chip drives patterned arrangement experiment of cardiomyocytes

During the experiment, neonatal rat cardiomyocytes were selected and placed in the microfluidic channel, and RF signals were applied to the IDT of the microfluidic chip. After the cardiomyocytes in the hydrogel were patterned, they were irradiated with ultraviolet light for 30s and the signal was turned off. Generator and power amplifier. Using X-ray microscope imaging technology to observe the hydrogel myocardial tissue fibers after curing is shown in Figure 13.

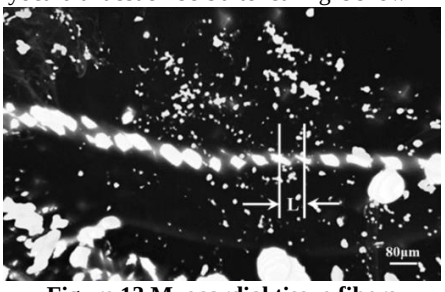

Figure 13 Myocardial tissue fibers

In the hydrogel myocardial tissue fibers formed after curing, the regularly arranged cardiomyocytes can be clearly seen (the marked part in Figure 13), which are driven to the nodes by the acoustic radiation force, and the distance L between adjacently arranged cardiomyocytes is The measurement is around 80μm, which accords with the theoretical value. This means that the surface acoustic wave microfluidic chip designed in this paper can pattern cardiomyocytes, and the established curing plan will not affect the distance between the directional arrangement of cardiomyocytes before and after curing, which can achieve the clinical application of myocardial tissue engineering. Patterning requirements.

5 Conclusion

In this study, a surface acoustic wave-based microfluidic chip technology was proposed for the patterned arrangement of cardiomyocytes, and a surface acoustic wave microfluidic chip with LiNbO3 as the piezoelectric substrate was fabricated. Using microparticles to complete the simulation experiment of surface acoustic wave driving the patterned arrangement of cardiomyocytes. The results show that when the glass capillary microtube is parallel to the interdigital, the line of the particles is parallel to the tube wall; when the glass tube and the interdigit are at an angle of 45° and 90°, the line of the patterned arrangement of the particles is perpendicular to the tube wall. Finally, a suitable hydrogel scaffold material was selected, and a surface acoustic wave microfluidic chip was used to arrange cardiomyocytes in the hydrogel. After curing the hydrogel, a theoretical result was obtained. It proves the high biocompatibility of surface acoustic wave and the great hope for the application of myocardial tissue engineering.

ACKNOWLEDGMENTS

The authors are grateful for the support provided by National Natural Science Foundation of China (No.52175545). Thanks to Professor Richard Fu for his careful guidance on this paper.

REFERENCES

[1] Jawad, H. , Ali, N. N. , Lyon, A.R. , Chen, Q. Z. , & Boccaccini, A. R. (2007). Myocardial tissue engineering: a review. Journal of Tissue Engineering and Regenerative Medicine, 1(5), 327-342.
[2] Ogle, B. M. , Bursac, N. , Domian, I. , Huang, N. F. , Menasche, P. , & Murry, C. E. , et al (2016). Distilling complexity to advance cardiac tissue engineering. Science Translational Medicine, 8(342), 342ps13.
[3] Engler, A. J. , Humbert, P. O. , Wehrle-Haller, B. , & Weaver, V. M. (2009). Multiscale modeling of form and function. Science, 324(5924), 208-212.
[4] Rivron, N. C. , Rouwkema, J. , R Truckenmüller, Karperien, M. , Boer, J. D. , & Blitterswijk, C. (2009). Tissue assembly and organization: developmental mechanisms in microfabricated tissues. Biomaterials, 30(28), 4851-4858.
[5] Li HY, Friend J, Yeo L, et al. (2009). Effect of surface acoustic waves on the viability, proliferation and differentiation of primary osteoblast-like cells. Biomicrofluidics, 3(3), 920.
[6] Wiklund, M. (2012). Acoustofluidics 12: Biocompatibility and cell viability in microfluidic acoustic resonators. Lab on a Chip, 12(11),2018-2028.
[7] Ruppel, C. , Reindl, L. , & Weigel, R. (2002). Saw devices and their wireless communications applications. Microwave Magazine IEEE, 3(2), 65-71.
[8] Collins, D. J. , Morahan, B. , Garcia-Bustos, J. , Doerig, C. , Plebanski, M. , & Neild, A. . (2015). Two-dimensional single-cell patterning with one cell per well driven by surface acoustic waves. Nature Communications, 6, 8686.
[9] Campbell, & C., K. . (1991). Applications of surface acoustic and shallow bulk acoustic wave devices. Modern Radar, 77(10), 1453-1484.